Charge-induced proton penetration across two-dimensional clay materials

Supplementary Information

Le Shi*, [1], Ao Xu[2], Zhixuan Ying[1], Yushuan Gao[1], Yonghong Cheng[1]

1. State Key Laboratory of Electrical Insulation and Power Equipment, Center of Nanomaterials for Renewable Energy, School of Electrical Engineering, Xi'an Jiaotong University, Xi'an 710049, China
2. School of Aeronautics, Northwestern Polytechnical University, Xi'an 710072, China

*Corresponding author. E-mail: le.shi@mail.xjtu.edu.cn (L. Shi)

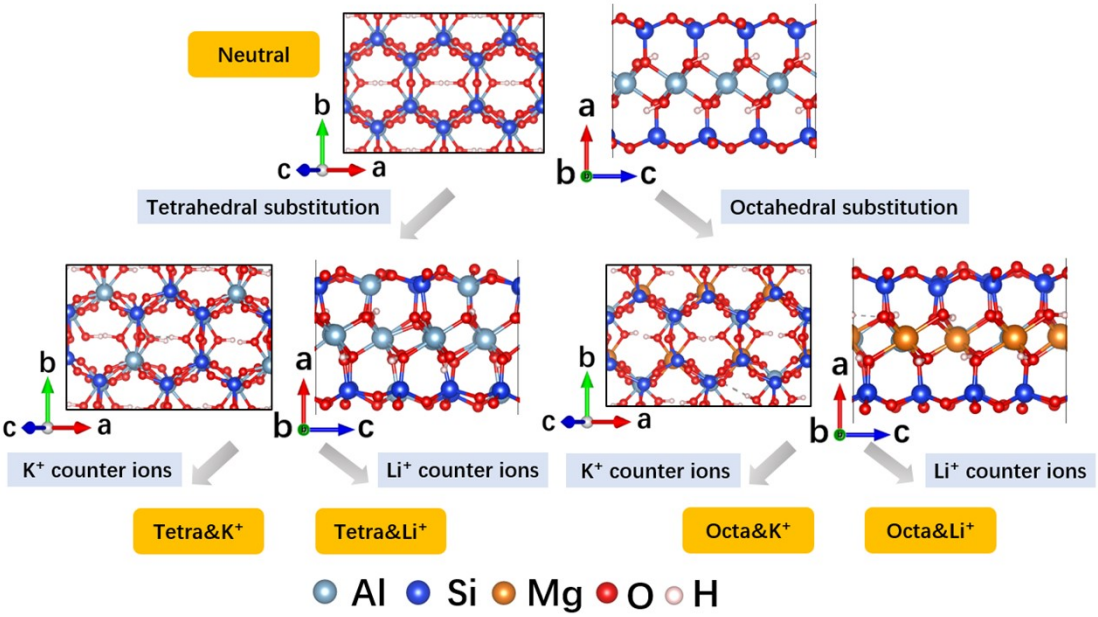

Fig. S1 Atomic structure of considered systems.

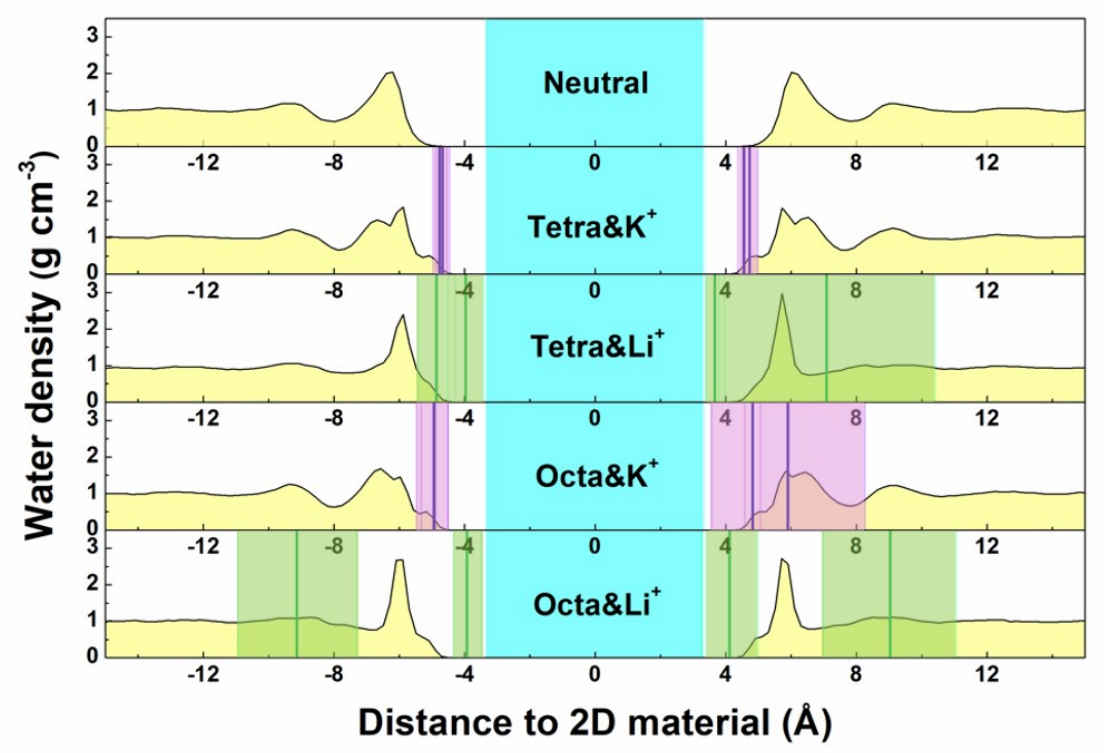

Fig. S2 Density profiles of water as a function of distance to 2D clay materials and the statistical position of K^+ (purple line and shade) and Li^+ (green line and shade) obtained from the classical MD trajectories. The cyan shade represents the position of 2D clay nanosheets.

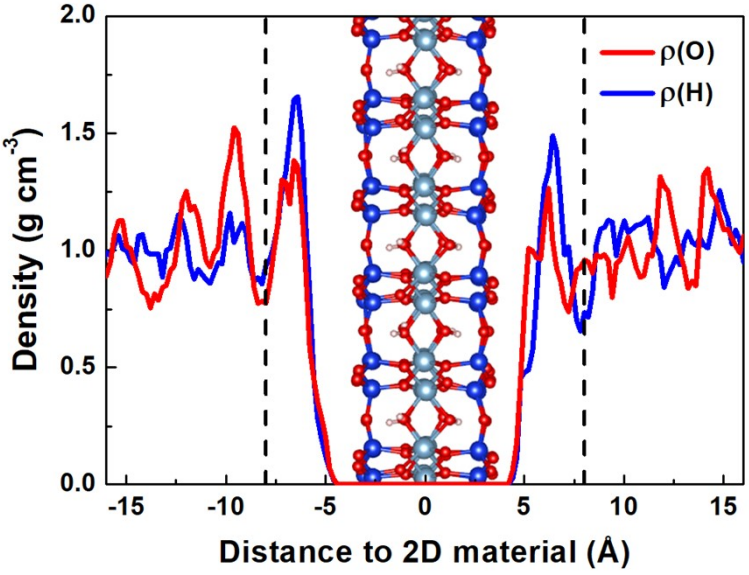

Fig. S3 Density profile of water as a function of distance to 2D clay material in "Neutral" system obtained from AIMD simulation.

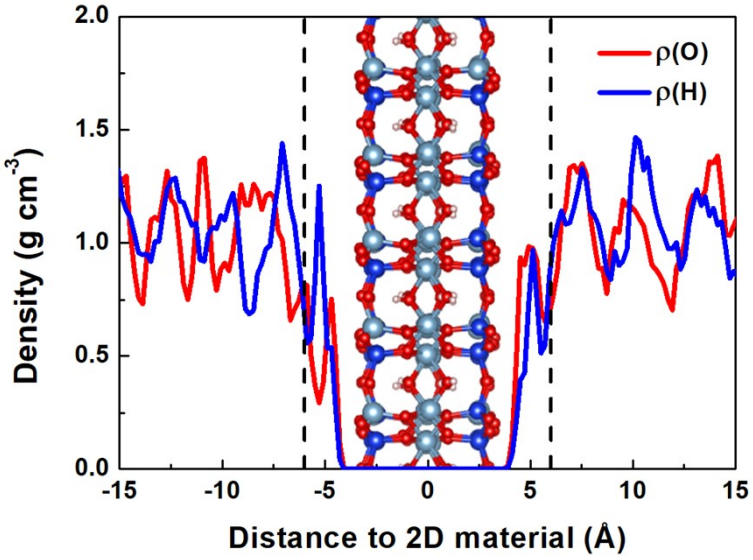

Fig. S4 Density profile of water as a function of distance to 2D clay material in "Tetra&K^+" system obtained from AIMD simulation.

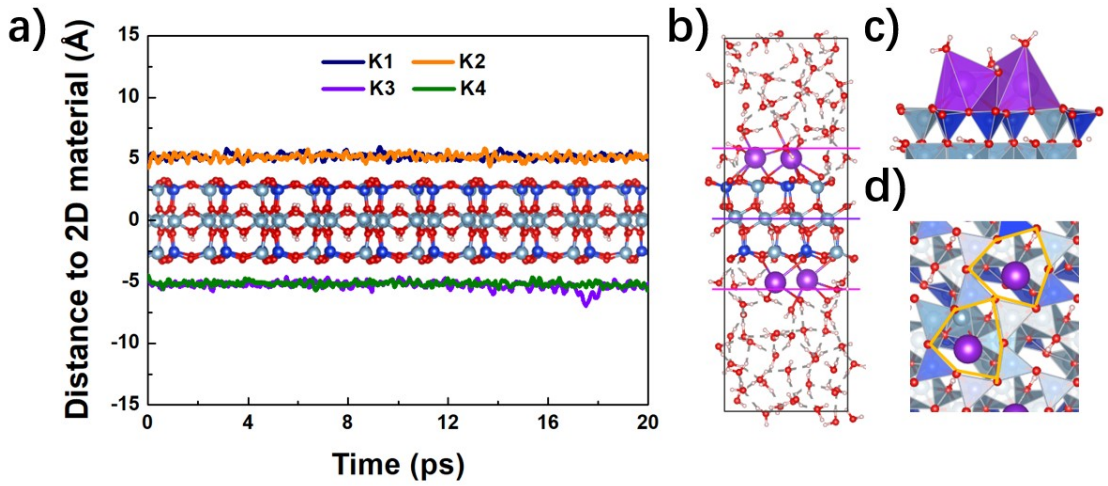

Fig. S5 a) Trajectories of K^+ during AIMD simulation for "Tetra&K^+" system. b) snapshot of "Tetra&K^+" system. c) side and d) top view of K^+ coordination environment

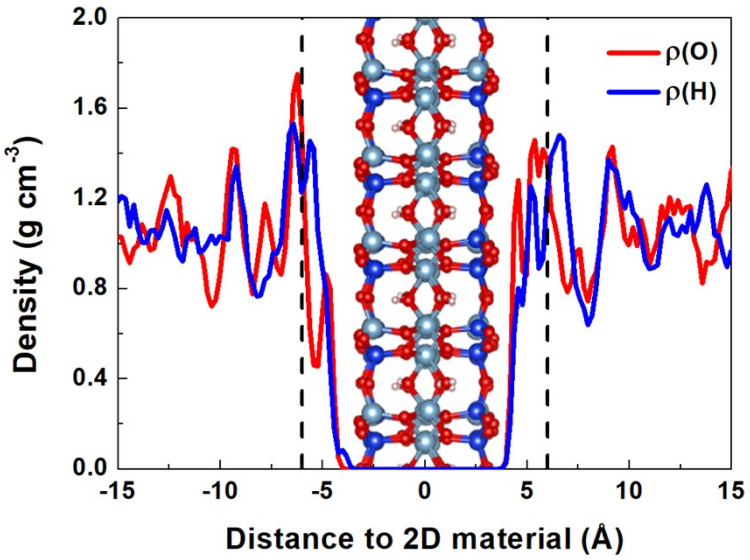

Fig. S6 Density profile of water as a function of distance to 2D clay material in "Tetra&Li^+" system obtained from AIMD simulation.

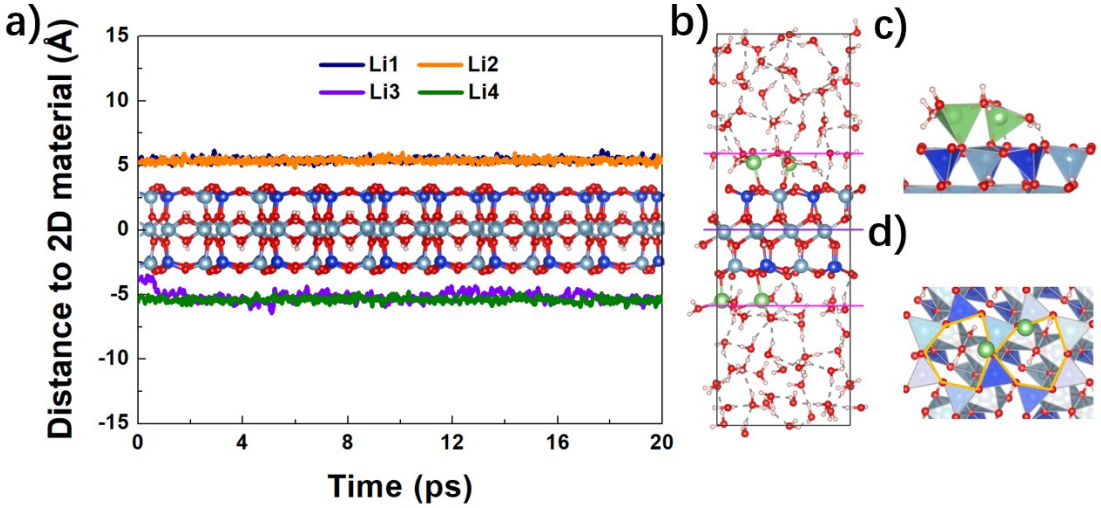

Fig. S7 a) Trajectories of Li^+ during AIMD simulation for "Tetra&Li^+" system. b) snapshot of "Tetra&Li^+" system. c) side and d) top view of Li^+ coordination environment

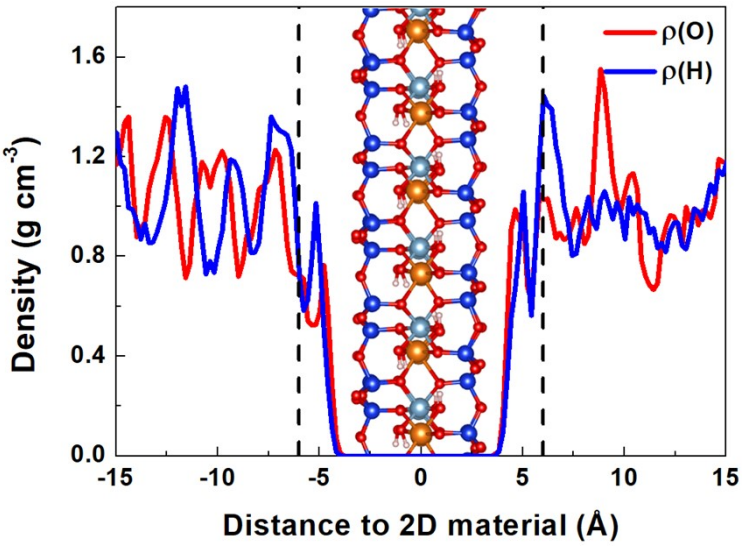

Fig. S8 Density profile of water as a function of distance to 2D clay material in "Octa&K^+" system obtained from AIMD simulation.

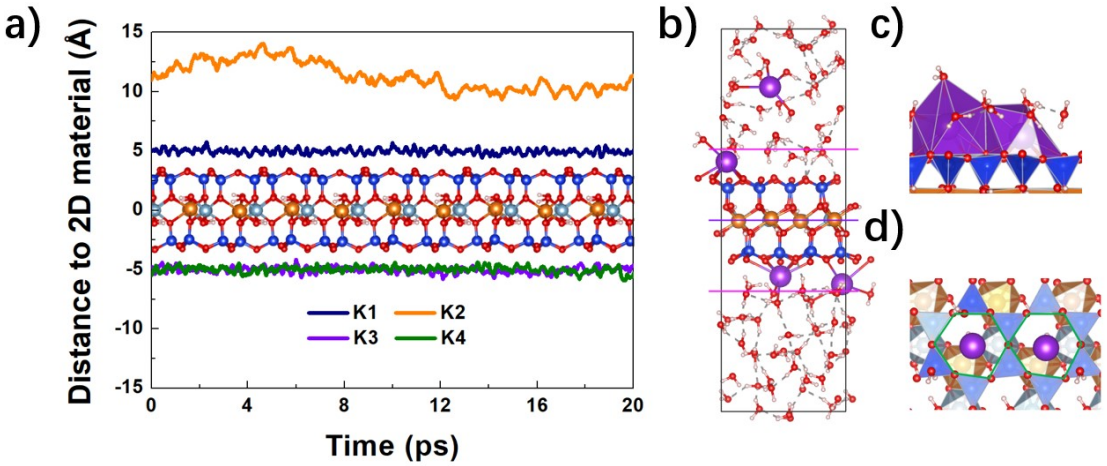

Fig. S9 a) Trajectories of K^+ during AIMD simulation for "Octa&K^+" system. b) snapshot of "Octa&K^+" system. c) side and d) top view of K^+ coordination environment

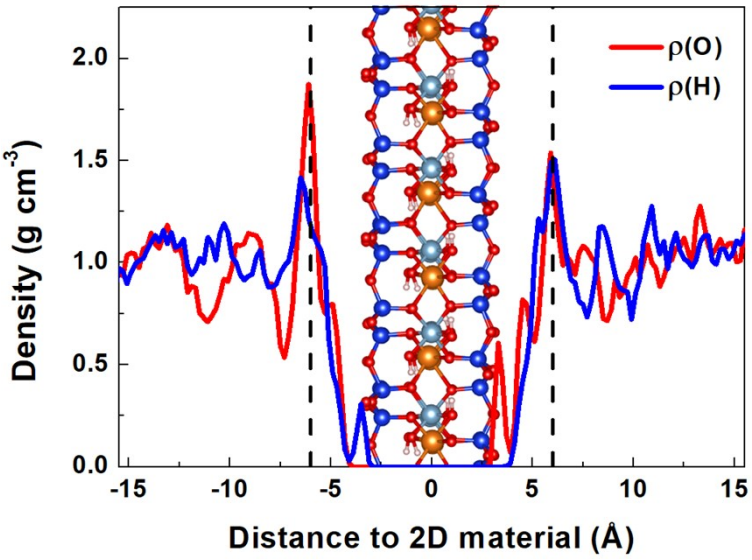

Fig. S10 Density profile of water as a function of distance to 2D clay material in "Octa&Li^+" system obtained from AIMD simulation.

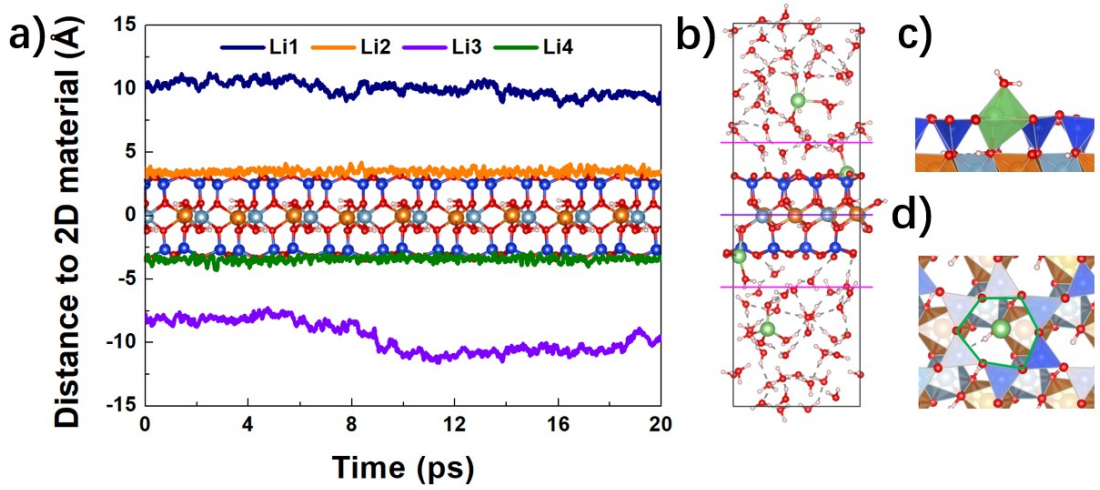

Fig. S11 a) Trajectories of Li^+ during AIMD simulation for "Octa&Li^+" system. b) snapshot of "Octa&Li^+" system. c) side and d) top view of Li^+ coordination environment

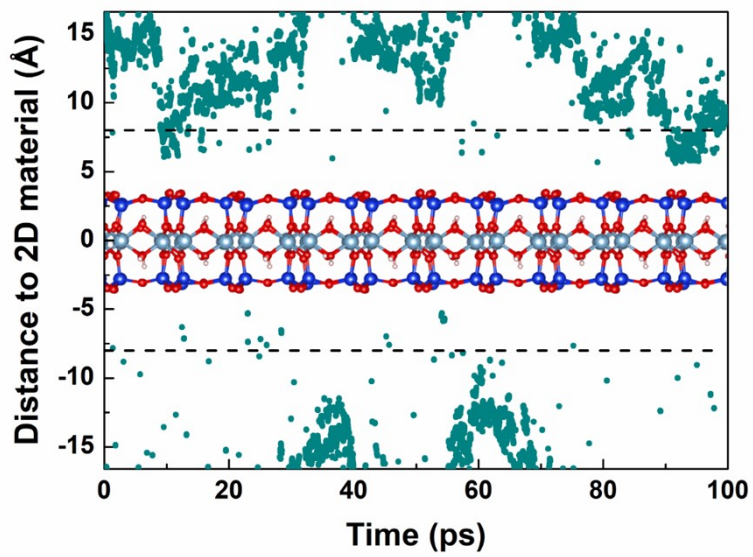

Fig. S12 The distance between proton and 2D clay material as a function of time in unbiased AIMD simulation for "Neutral" system

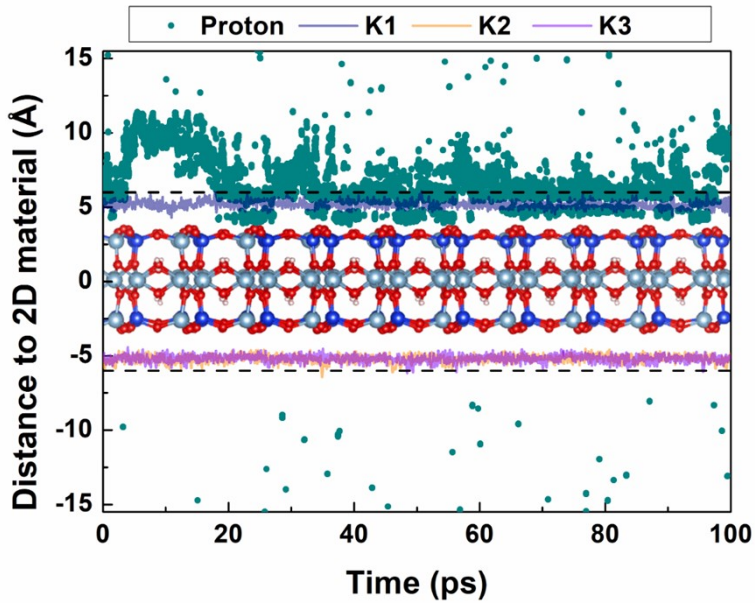

Fig. S13 The distance between proton, K^+ ions and 2D clay material as a function of time in unbiased AIMD simulation for "Tetra&K^+" system

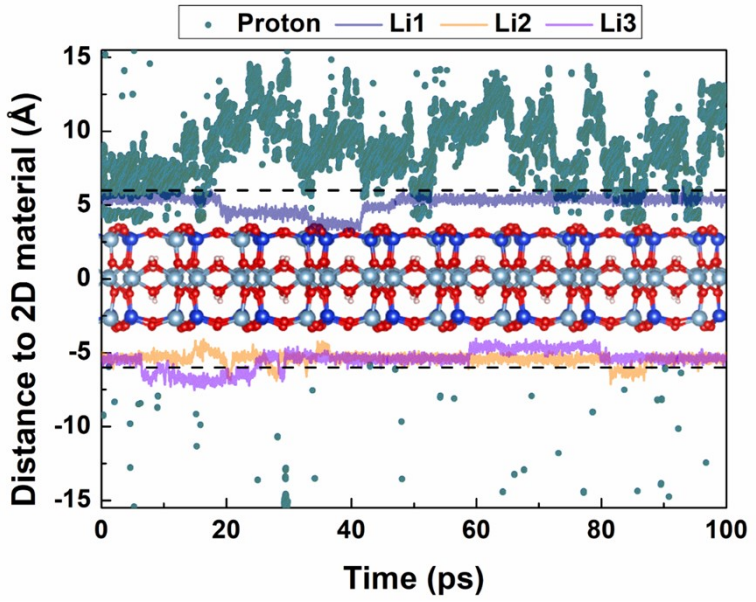

Fig. S14 The distance between proton, Li^+ ions and 2D clay material as a function of time in unbiased AIMD simulation for "Tetra&Li^+" system

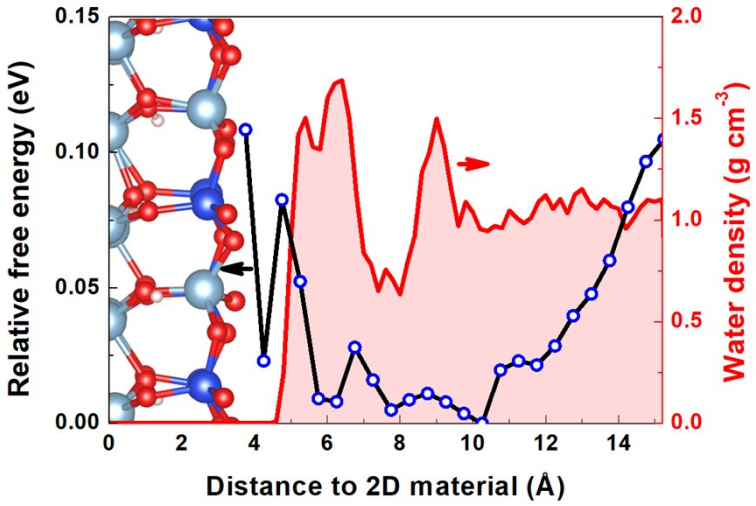

Fig. S15 Proton energy profile (black line with blue circle) and water density profile (redline with a pink shade) as a function of distance to 2D clay material in "Tetra&Li^+" system

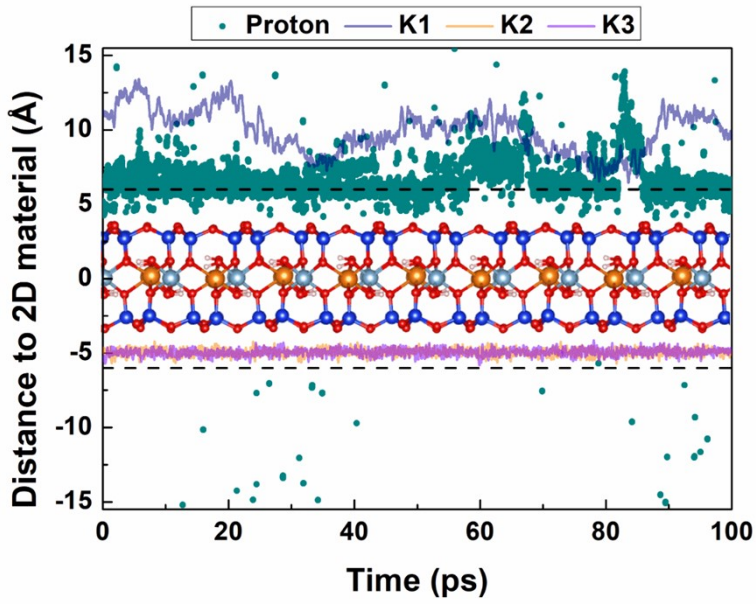

Fig. S16 The distance between proton, K^+ ions and 2D clay material as a function of time in unbiased AIMD simulation for "Octa&K^+" system

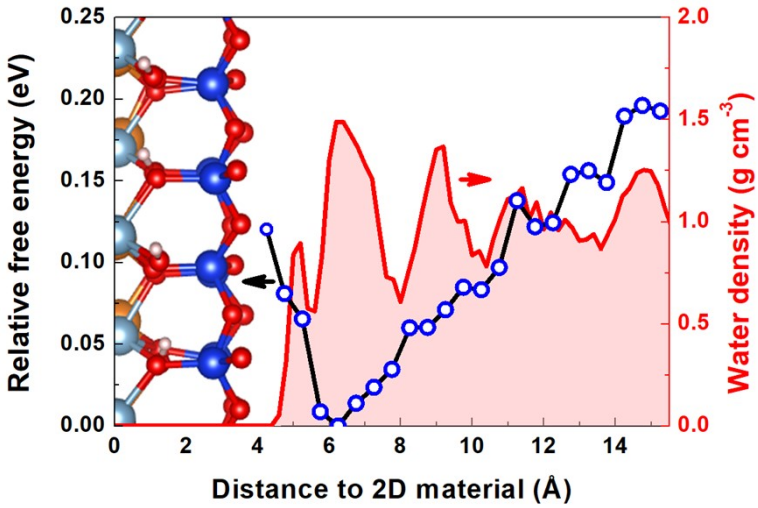

Fig. S17 Proton energy profile (black line with blue circle) and water density profile (redline with a pink shade) as a function of distance to 2D clay material in "Octa&K^+" system

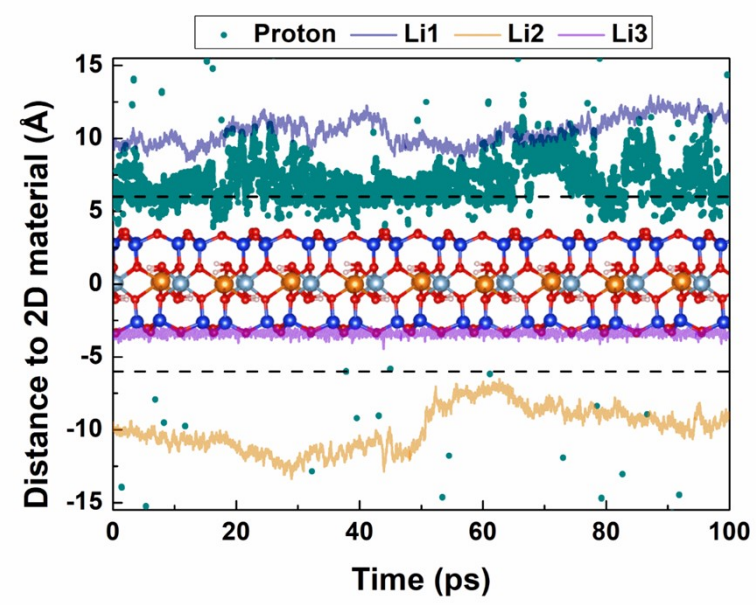

Fig. S18 The distance between proton, Li^+ ions and 2D clay material as a function of time in unbiased AIMD simulation for "Octa&Li^+" system

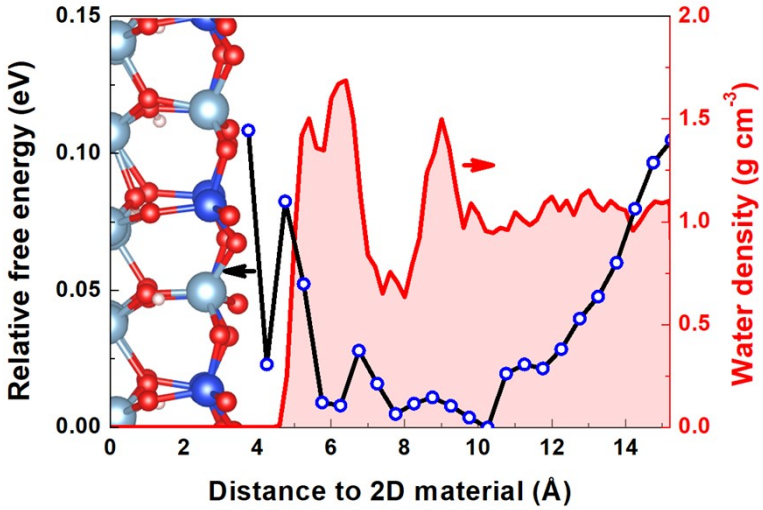

Fig. S19 Proton energy profile (black line with blue circle) and water density profile (redline with a pink shade) as a function of distance to 2D clay material in "Octa&Li^+" system

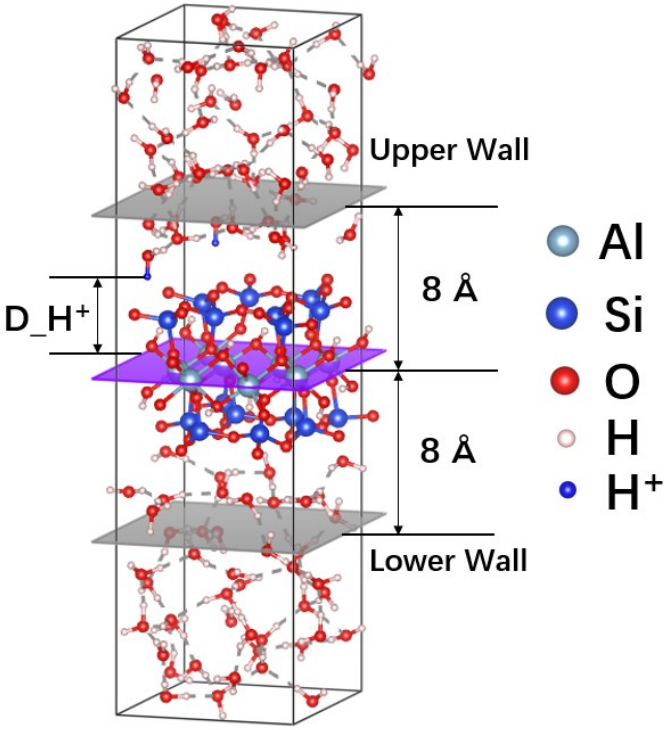

Fig. S20 Setup for metadynamics simulations of proton penetration across 2D clay material with constraints in "Neutral" system.

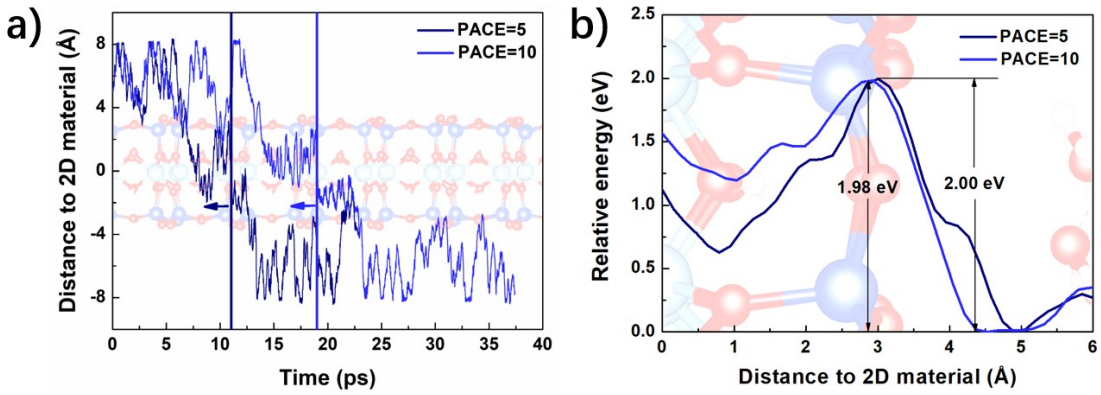

Fig. S21 a) Distance between the proton and 2D clay material as a function of time in metadynamics simulations with different deposition pace and b) the corresponding energy profiles of proton in "Neutral" system.

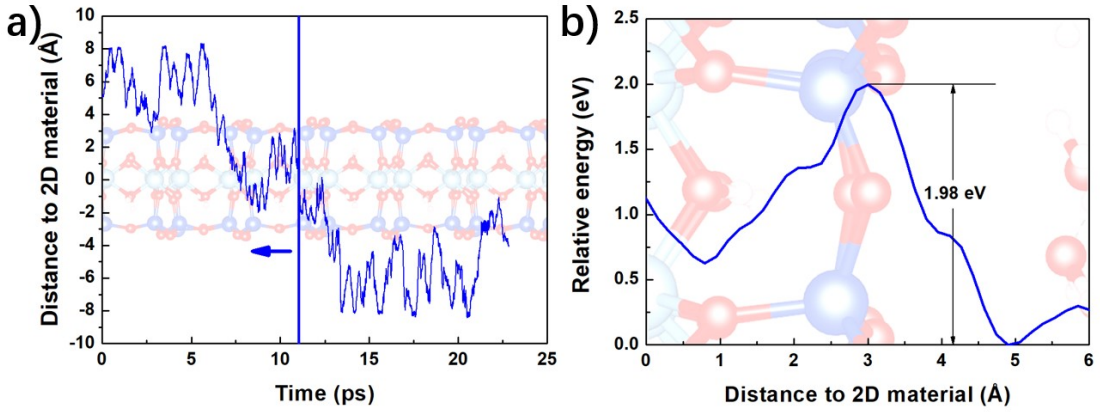

Fig. S22 a) Distance between the proton and 2D clay material as a function of time in metadynamics simulation and b) the corresponding energy profile of proton in "Neutral" system with #1 initial geometry

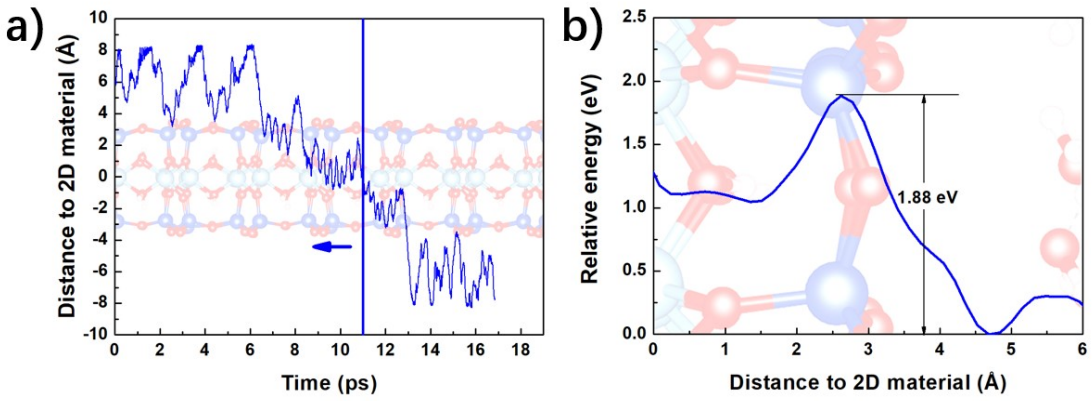

Fig. S23 a) Distance between the proton and 2D clay material as a function of time in metadynamics simulation and b) the corresponding energy profile of proton in "Neutral" system with #2 initial geometry

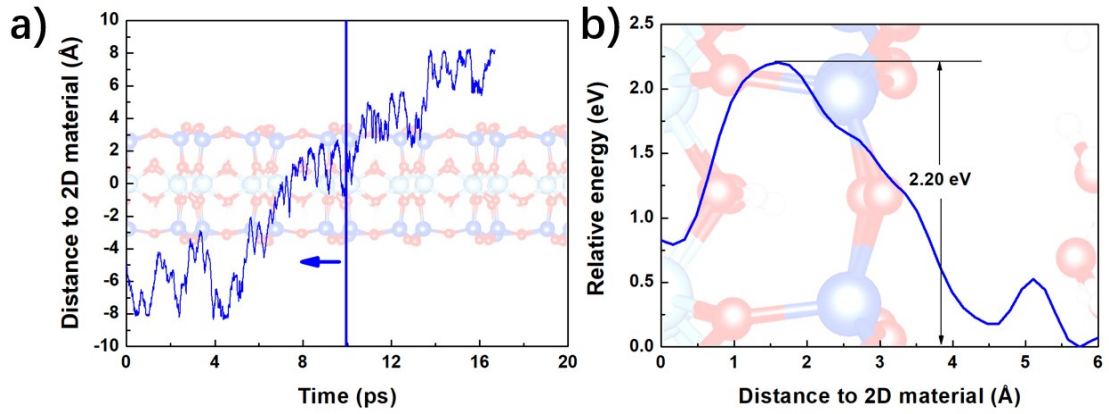

Fig. S24 a) Distance between the proton and 2D clay material as a function of time in metadynamics simulation and b) the corresponding energy profile of proton in "Neutral" system with #3 initial geometry

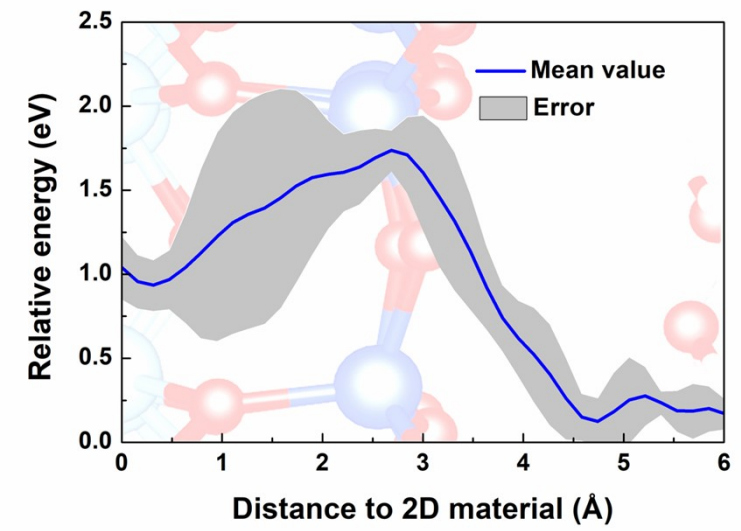

Fig. S25 Averaged free energy profile of proton in "Neutral" system calculated from three metadynamics runs with different initial geometries

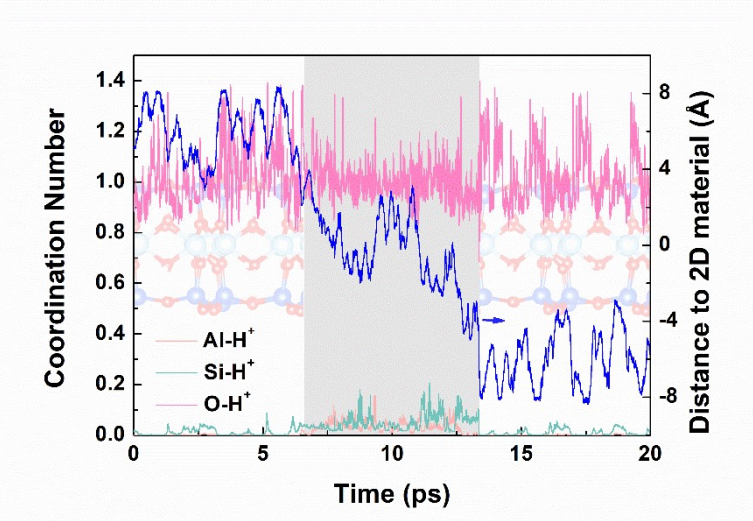

Fig.S26 Distance between the proton and 2D clay material, Al-H^+, Si-H^+ and O-H^+ coordination number as a function of simulation time in #1 metadynamics simulation of proton penetration across 2D clay material for "Neutral" system.

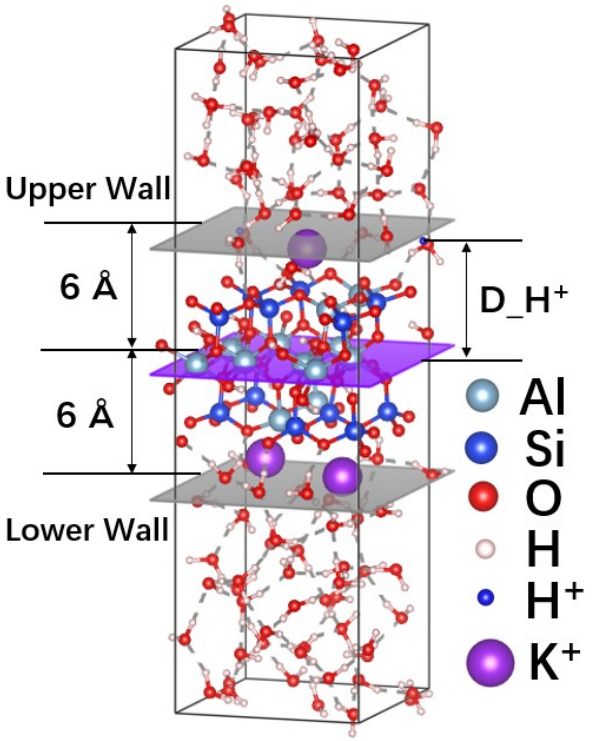

Fig.S27 Setup for metadynamics simulations of proton penetration across 2D clay material with constraints in "Tetra&K^+" system

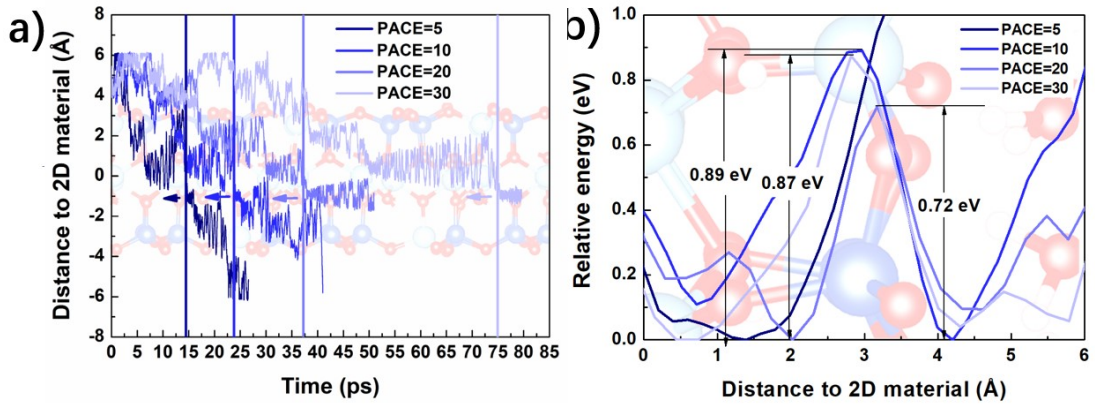

Fig. S28 a) Distance between the proton and 2D clay material as a function of time in metadynamics simulations with different deposition pace and b) the corresponding energy profiles of proton in "Tetra&K^+" system.

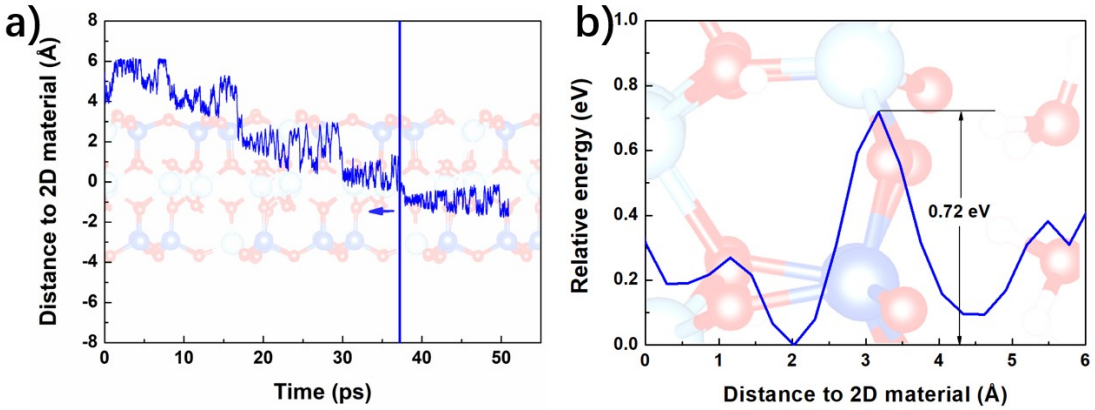

Fig. S29 a) Distance between the proton and 2D clay material as a function of time in metadynamics simulation and b) the corresponding energy profile of proton in "Tetra&K^+" system with #1 initial geometry

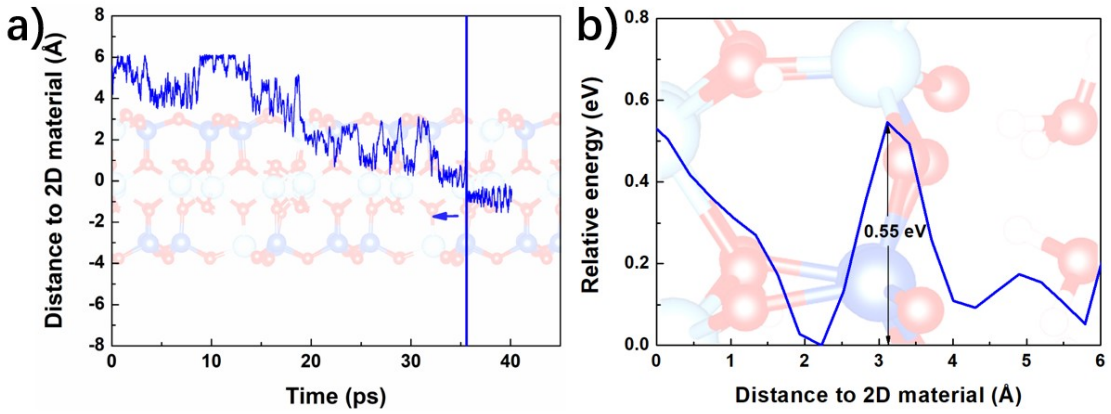

Fig. S30 a) Distance between the proton and 2D clay material as a function of time in metadynamics simulation and b) the corresponding energy profile of proton in "Tetra&K^+" system with #2 initial geometry

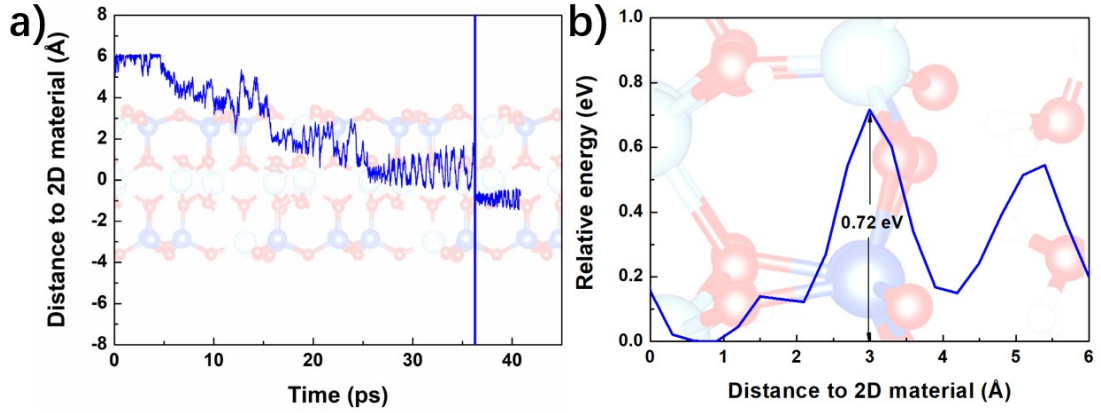

Fig. S31 a) Distance between the proton and 2D clay material as a function of time in metadynamics simulation and b) the corresponding energy profile of proton in "Tetra&K^+" system with #3 initial geometry

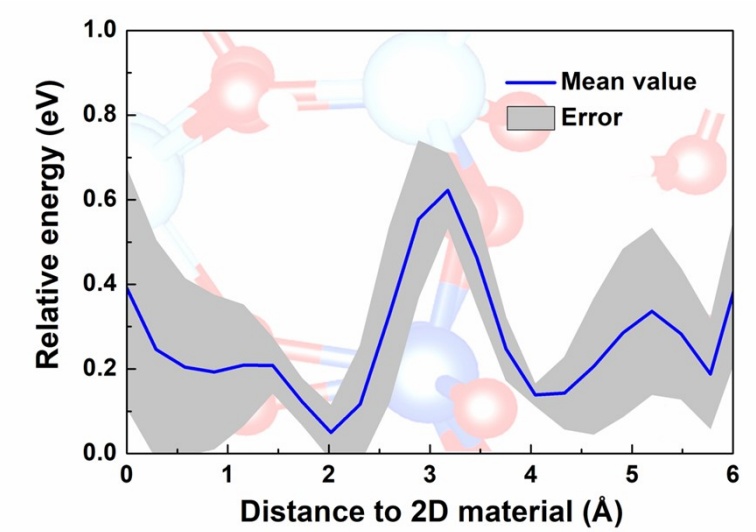

Fig. S32 Averaged free energy profile of proton in "Tetra&K" system calculated from three metadynamics runs with different initial geometries.

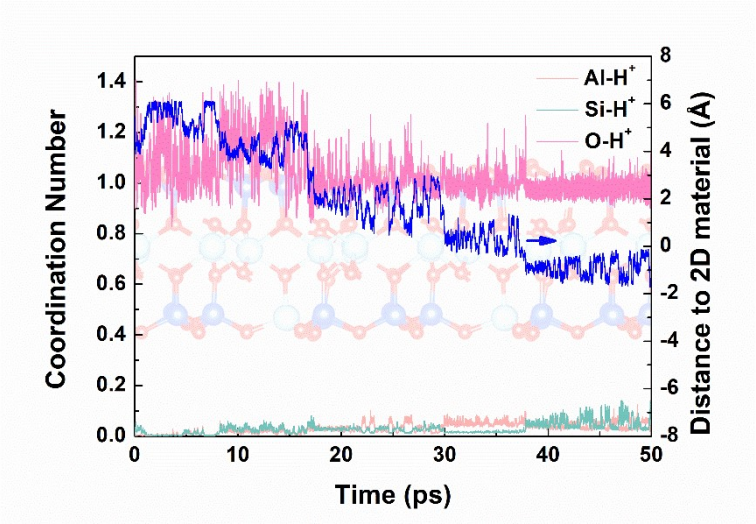

Fig. S33 Distance between the proton and 2D clay material, Al-H^+, Si-H^+ and O-H^+ coordination number as a function of simulation time in #1 metadynamics simulation of proton penetration across 2D clay material for "Tetra&K^+" system.

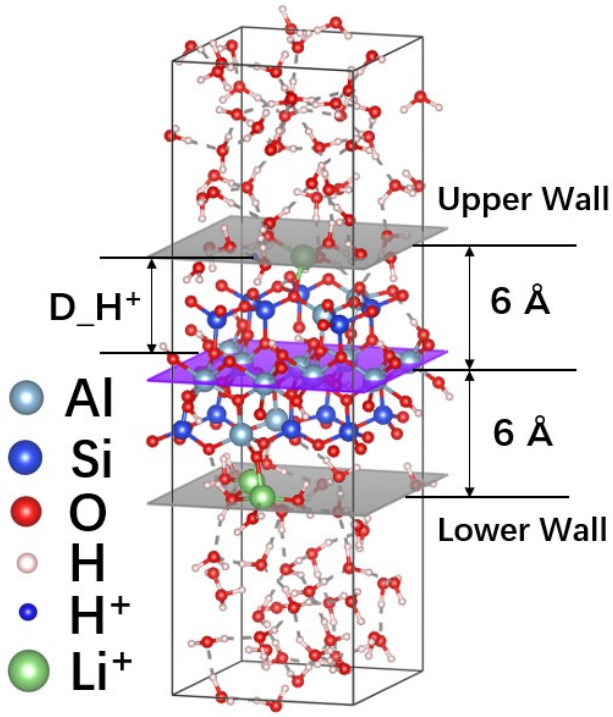

Fig. S34 Setup for metadynamics simulations of proton penetration across 2D clay material with constraints in "Tetra&Li^+" system

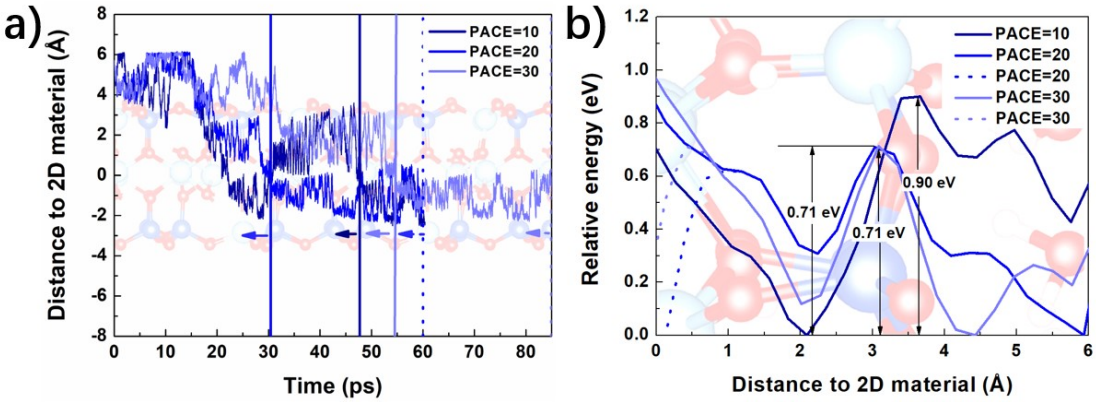

Fig. S35 a) Distance between the proton and 2D clay material as a function of time in metadynamics simulations with different deposition pace and b) the corresponding energy profiles of proton in "Tetra&Li^+" system.

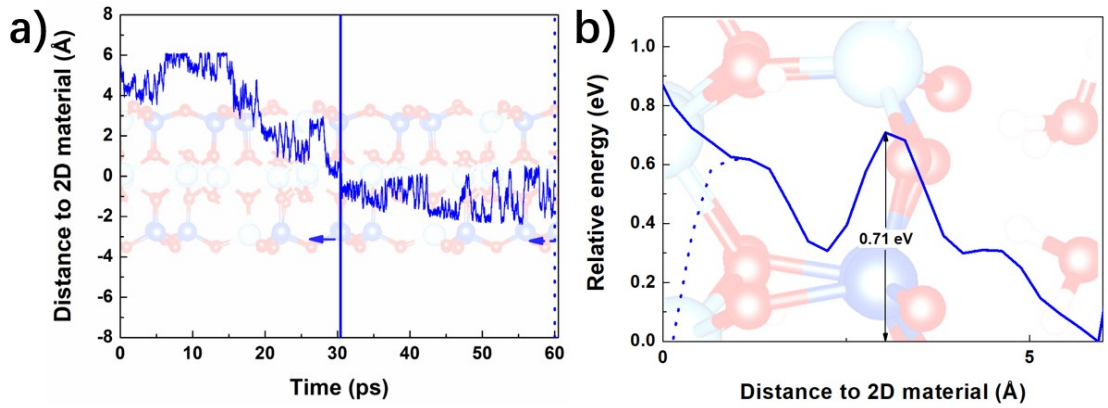

Fig. S36 a) Distance between the proton and 2D clay material as a function of time in metadynamics simulation and b) the corresponding energy profile of proton in "Tetra&Li^+" system with #1 initial geometry

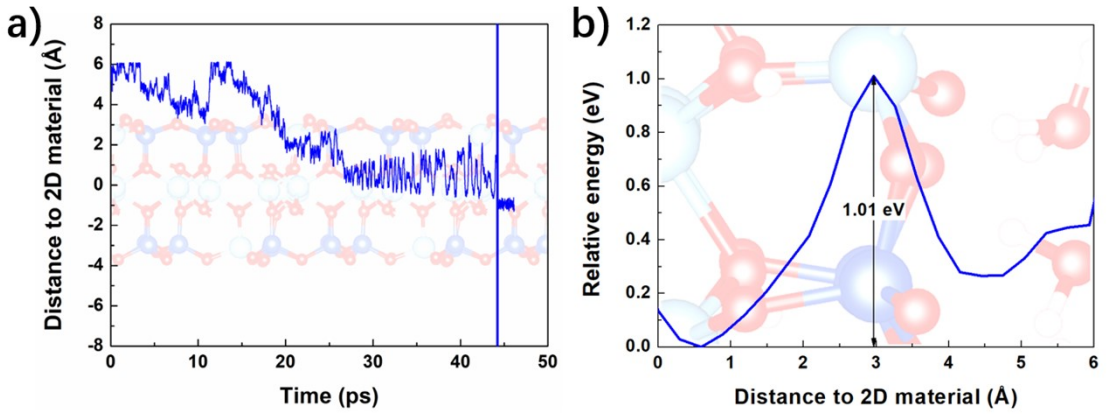

Fig. S37 a) Distance between the proton and 2D clay material as a function of time in metadynamics simulation and b) the corresponding energy profile of proton in "Tetra&Li^+" system with #2 initial geometry

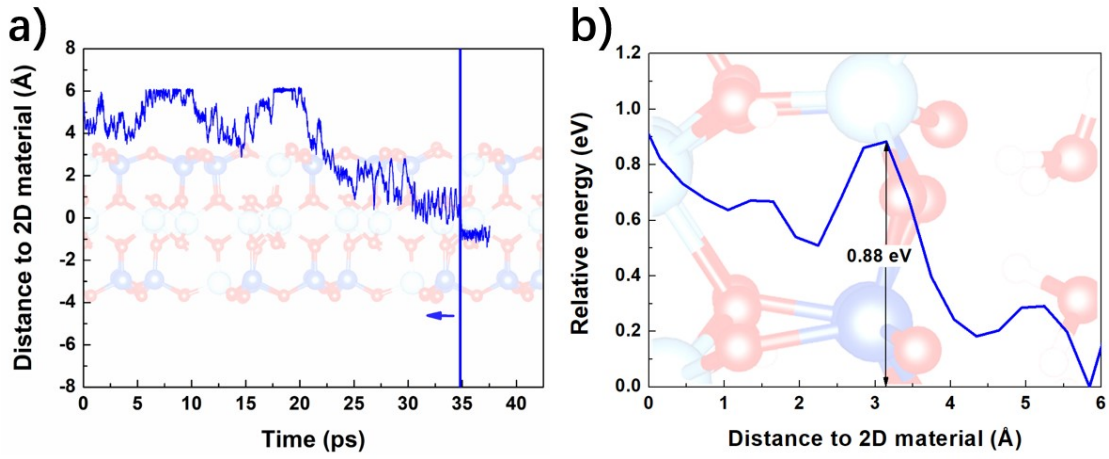

Fig. S38 a) Distance between the proton and 2D clay material as a function of time in metadynamics simulation and b) the corresponding energy profile of proton in "Tetra&Li^+" system with #3 initial geometry

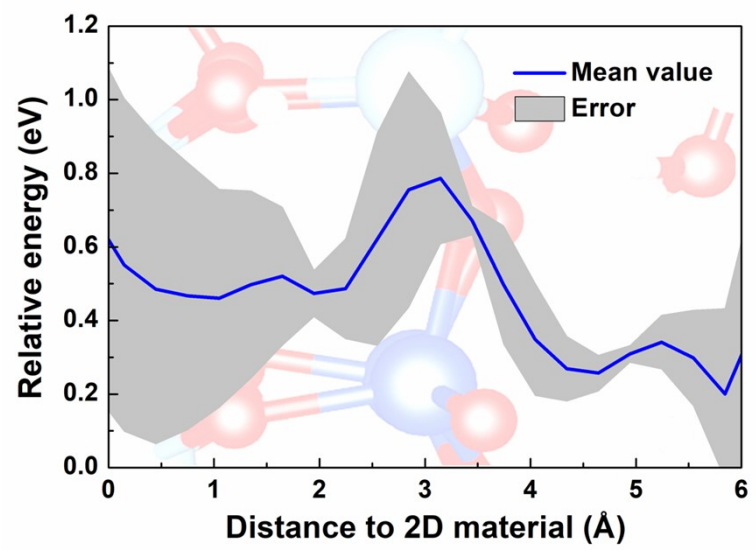

Fig. S39 Averaged free energy profile of proton in "Tetra&Li^+" system calculated from three metadynamics runs with different initial geometries.

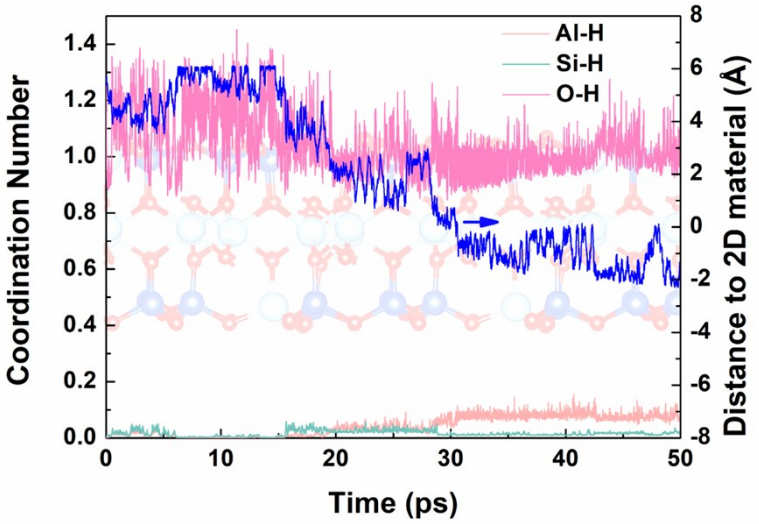

Fig. S40 Distance between the proton and 2D clay material, Al-H^+, Si-H^+ and O-H^+ coordination number as a function of simulation time in #1 metadynamics simulation of proton penetration across 2D clay material for "Tetra&Li^+" system.

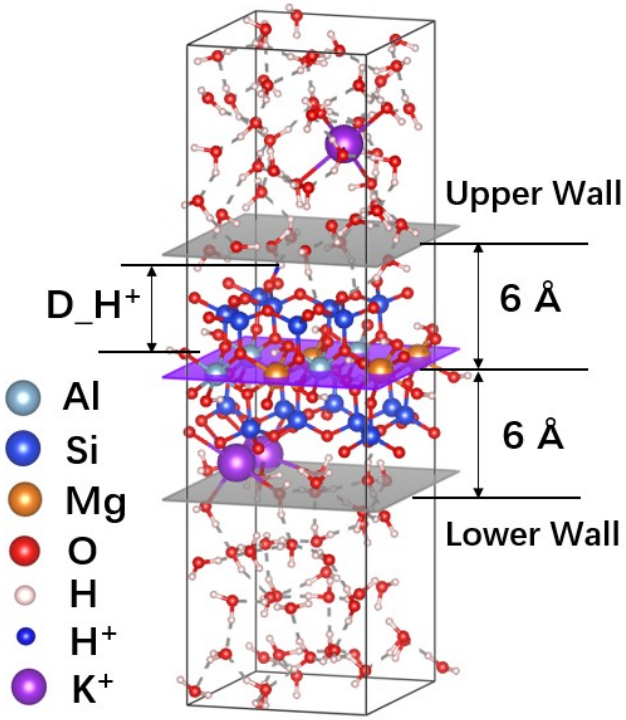

Fig. S41 Setup for metadynamics simulations of proton penetration across 2D clay material with constraints in "Octa&K^+" system

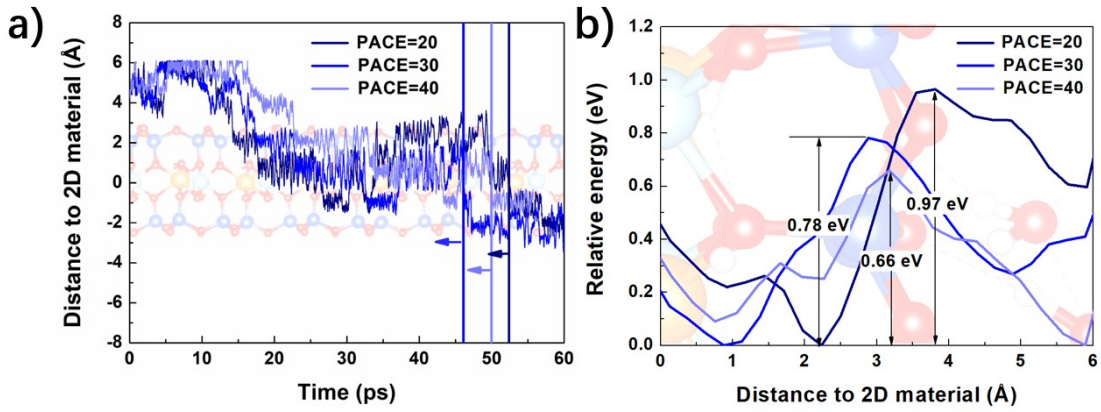

Fig. S42 a) Distance between the proton and 2D clay material as a function of time in metadynamics simulations with different deposition pace and b) the corresponding energy profiles of proton in "Octa&K^+" system.

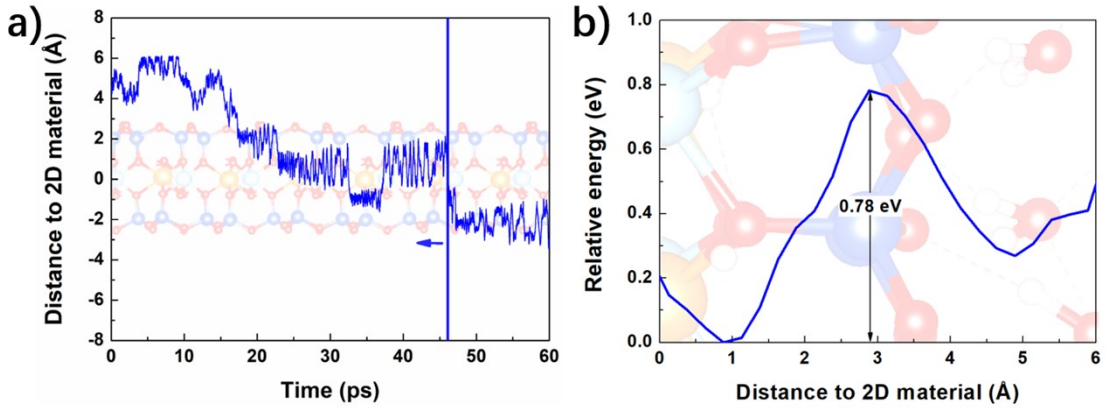

Fig. S43 a) Distance between the proton and 2D clay material as a function of time in metadynamics simulation and b) the corresponding energy profile of proton in "Octa&K^+" system with #1 initial geometry

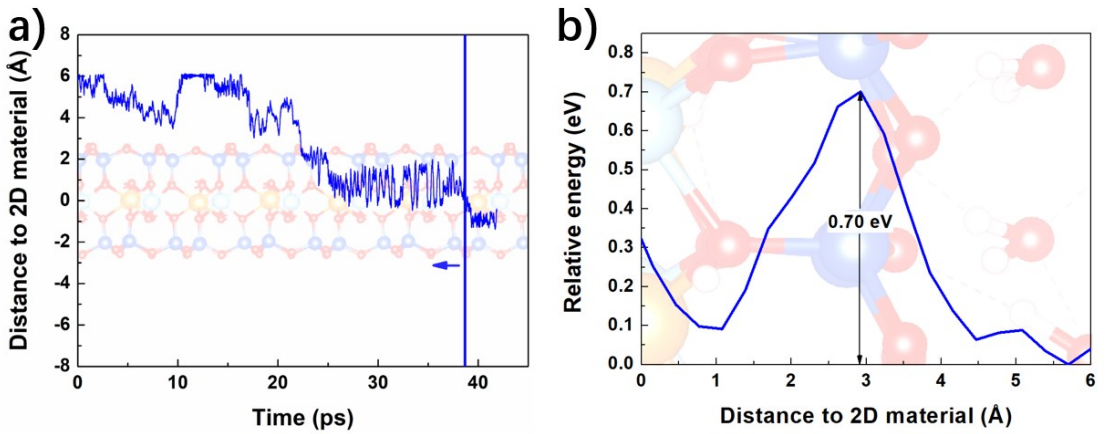

Fig. S44 a) Distance between the proton and 2D clay material as a function of time in metadynamics simulation and b) the corresponding energy profile of proton in "Octa&K^+" system with #2 initial geometry

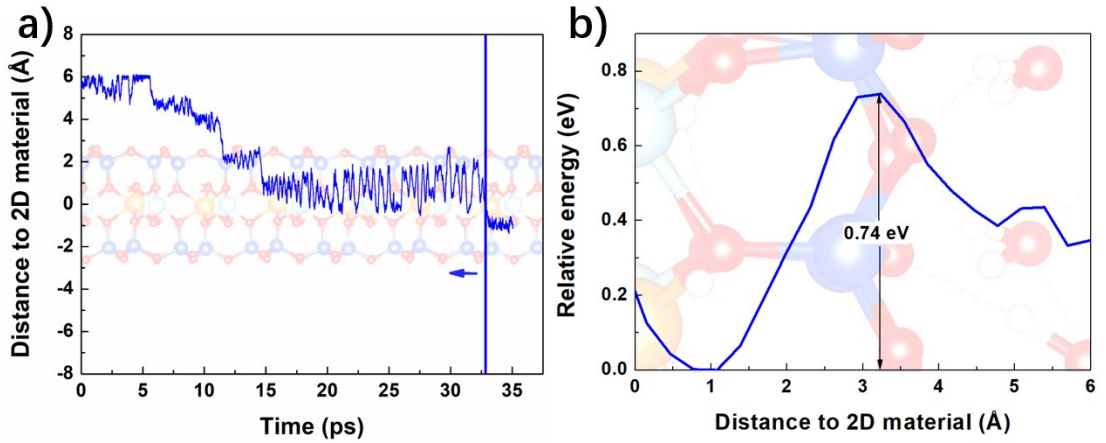

Fig. S45 a) Distance between the proton and 2D clay material as a function of time in metadynamics simulation and b) the corresponding energy profile of proton in "Octa&K^+" system with #3 initial geometry

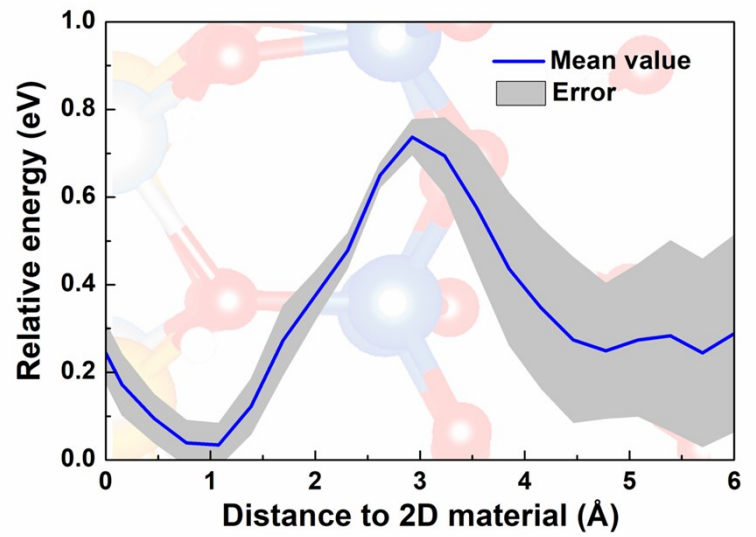

Fig. S46 Averaged free energy profile of proton in "Octa&K" system calculated from three metadynamics runs with different initial geometries.

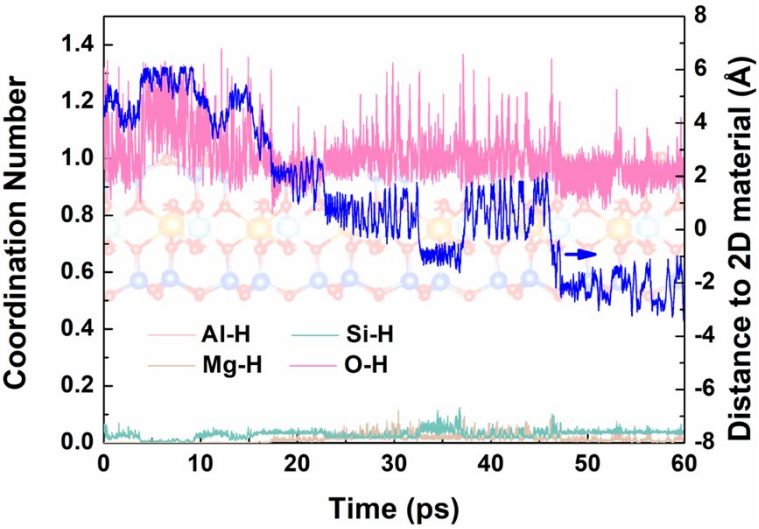

Fig. S47 Distance between the proton and 2D clay material, Al-H^+, Mg-H^+, Si-H^+ and O-H^+ coordination number as a function of simulation time in #1 metadynamics simulation of proton penetration across 2D clay material for "Octa&K^+" system.

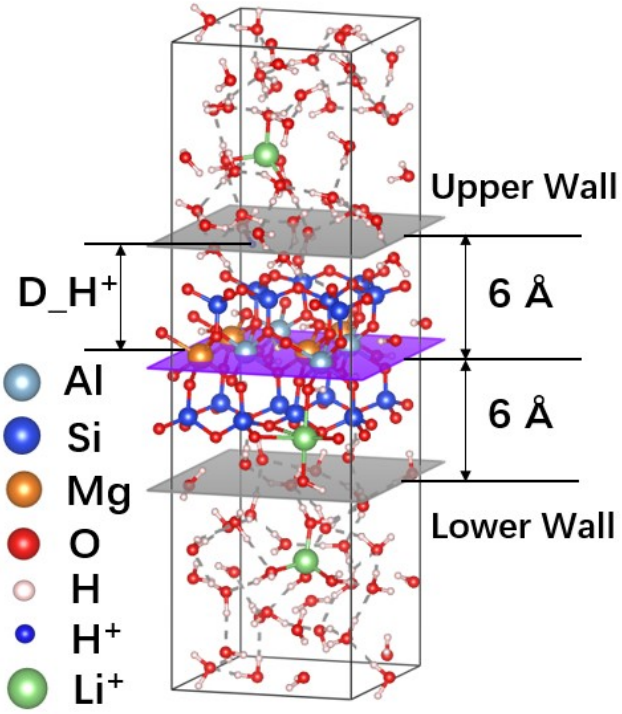

Fig. S48 Setup for metadynamics simulations of proton penetration across 2D clay material with constraints in "Octa&Li^+" system

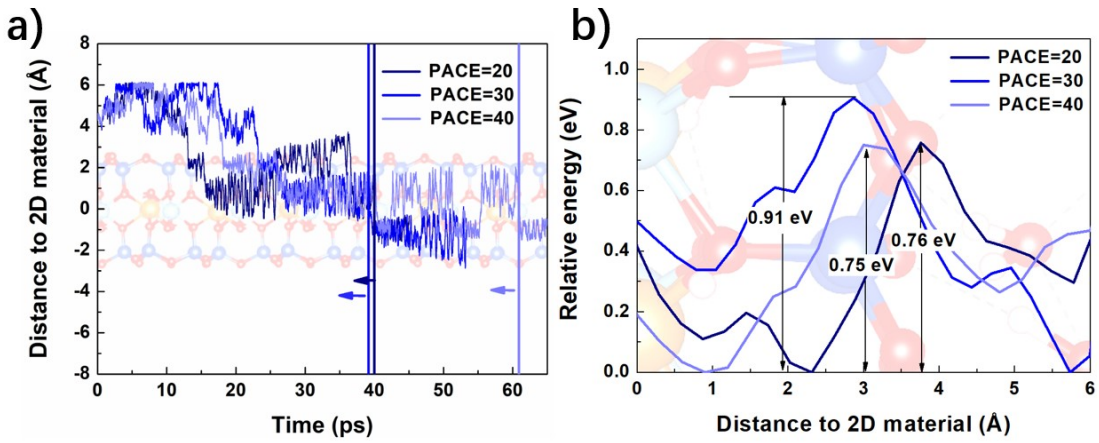

Fig. S49 a) Distance between the proton and 2D clay material as a function of time in metadynamics simulations with different deposition pace and b) the corresponding energy profiles of proton in Octa&Li^+ system.

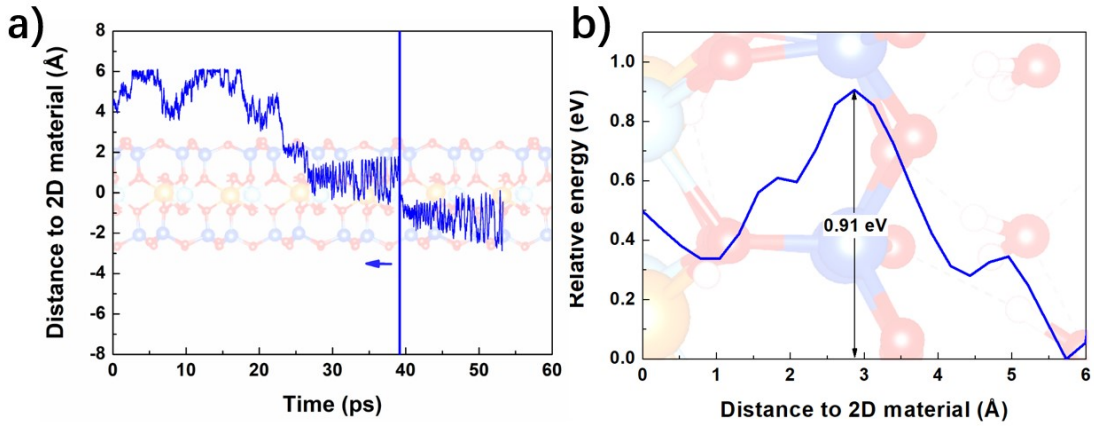

Fig. S50 a) Distance between the proton and 2D clay material as a function of time in metadynamics simulation and b) the corresponding energy profile of proton in Octa&Li^+ system with #1 initial geometry

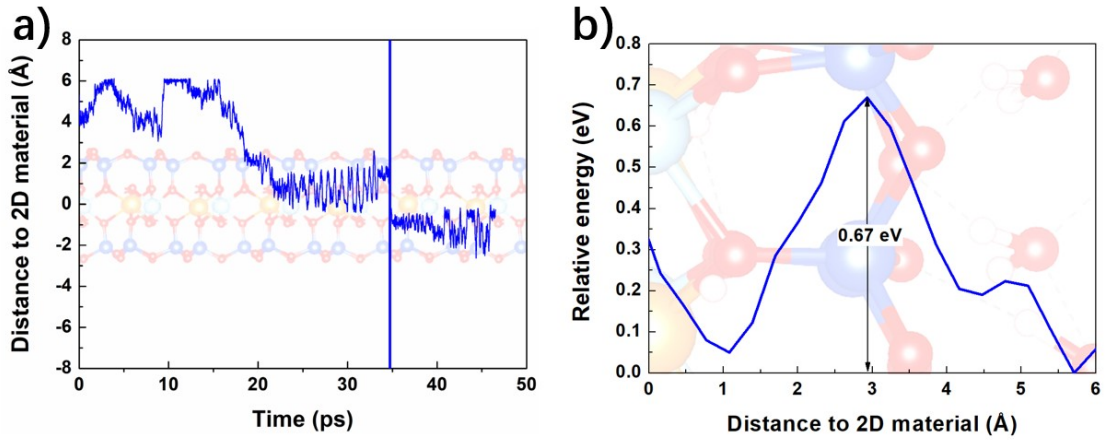

Fig. S51 a) Distance between the proton and 2D clay material as a function of time in metadynamics simulation and b) the corresponding energy profile of proton in Octa&Li^+ system with #2 initial geometry

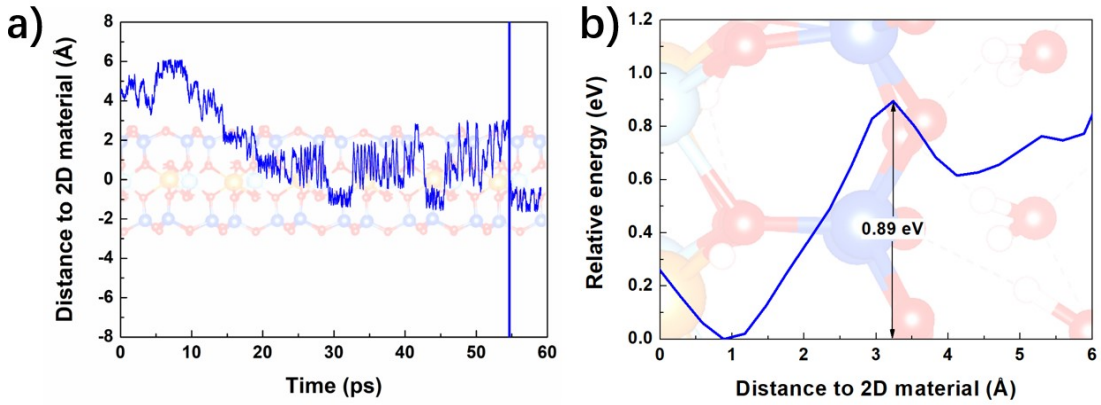

Fig. S52 a) Distance between the proton and 2D clay material as a function of time in metadynamics simulation and b) the corresponding energy profile of proton in Octa&Li^{+} system with #3 initial geometry

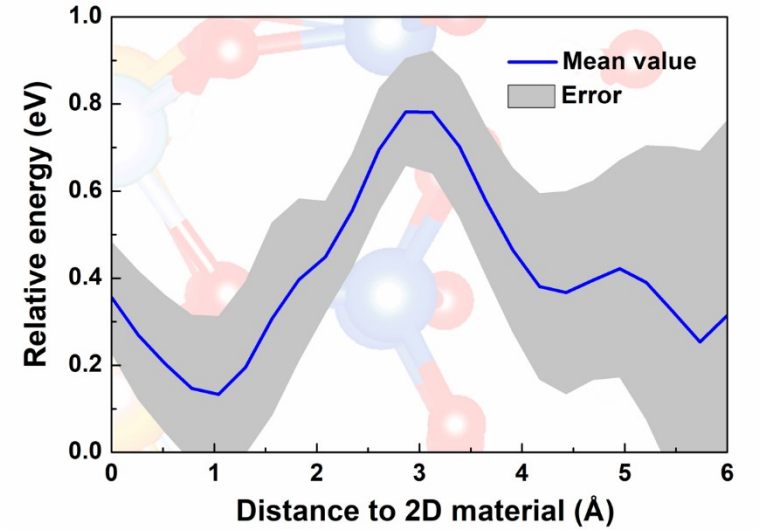

Fig. S53 Averaged free energy profile of proton in "Octa&Li" system calculated from three metadynamics runs with different initial geometries.

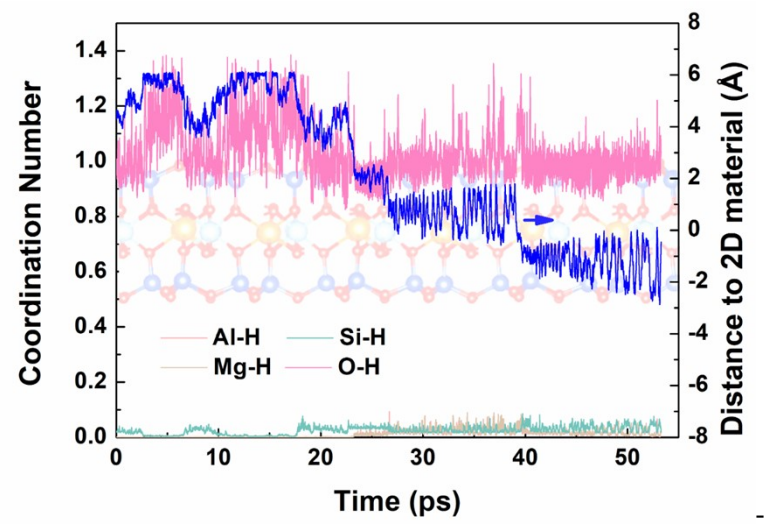

Fig. S54 Distance between the proton and 2D clay material, Al-H^+, Mg-H^+, Si-H^+ and O-H^+ coordination number as a function of simulation time in #1 metadynamics simulation of proton penetration across 2D clay material for Octa&Li^+ system.

Table S1. Simulation setups for two-dimensional clay materials in aqueous environment

	a (Å)	b (Å)	c (Å)	N_{water}	ρ_{water} (g cm^{-3})
Neutral	10.42	9.03	33.19	74	0.89
Tetra&K^+	10.51	9.13	31.77	74	0.93
Tetra&Li^+	10.51	9.13	30.86	74	0.96
Octa&K^+	10.51	9.13	32.34	74	0.91
Octa&Li^+	10.51	9.13	31.79	74	0.93

Table S2 Deposition pace convergence test for proton penetration across 2D clay materials with constraints

Pace		5	10	20	30	40
Energy barrier (eV)	Neutral	2.00	1.98	/	/	/
	Tetra&K^+	1.26	0.89	0.72	0.87	/
	Tetra&Li^+	/	0.90	0.71	0.71	/
	Octa&K^+	/	/	0.97	0.78	0.66
	Octa&Li^+	/	/	0.91	0.76	0.75

Table S3 Calculated proton penetration energy barriers with different initial geometries

Initial geometry		#1	#2	#3	Average
Energy barrier (eV)	Neutral	1.98	1.88	2.20	2.02±0.16
	Tetra&K^+	0.72	0.55	0.72	0.66±0.10
	Tetra&Li^+	0.71	1.01	0.88	0.87±0.15
	Octa&K^+	0.78	0.70	0.74	0.74±0.04
	Octa&Li^+	0.91	0.67	0.89	0.82±0.13

Table S4 Parameters adopted for the production run of metadynamics simulations

	Pace (timestep)	Height (KJ mol^{-1})	Sigma (Å)
Neutral	5	1	0.25
Tetra&K^+	20	0.2	0.25
Tetra&Li^+	20	0.2	0.25
Octa&K^+	30	0.2	0.25
Octa&Li^+	30	0.2	0.25